Biointerphases
A Journal of Biomaterials and Biological Interfaces

How do plasma-generated OH radicals react with biofilm components? Insights from atomic scale simulations

Narjes Khosravian, Annemie Bogaerts, Stijn Huygh, Maksudbek Yusupov, and Erik C. Neyts

Citation: Biointerphases **10**, 029501 (2015); doi: 10.1116/1.4904339
View online: http://dx.doi.org/10.1116/1.4904339
View Table of Contents: http://scitation.aip.org/content/avs/journal/bip/10/2?ver=pdfcov
Published by the AVS: Science & Technology of Materials, Interfaces, and Processing

How do plasma-generated OH radicals react with biofilm components? Insights from atomic scale simulations

Narjes Khosravian, Annemie Bogaerts, Stijn Huygh, Maksudbek Yusupov, and Erik C. Neyts[a)]
Research Group PLASMANT, Department of Chemistry, University of Antwerp, Universiteitsplein 1, B-2610 Antwerp, Belgium

(Received 31 October 2014; accepted 4 December 2014; published 17 December 2014)

The application of nonthermal atmospheric pressure plasma is emerging as an alternative and efficient technique for the inactivation of bacterial biofilms. In this study, reactive molecular dynamics simulations were used to examine the reaction mechanisms of hydroxyl radicals, as key reactive oxygen plasma species in biological systems, with several organic molecules (i.e., alkane, alcohol, carboxylic acid, and amine), as prototypical components of biomolecules in the biofilm. Our results demonstrate that organic molecules containing hydroxyl and carboxyl groups may act as trapping agents for the OH radicals. Moreover, the impact of OH radicals on *N*-acetyl-glucosamine, as constituent component of staphylococcus epidermidis biofilms, was investigated. The results show how impacts of OH radicals lead to hydrogen abstraction and subsequent molecular damage. This study thus provides new data on the reaction mechanisms of plasma species, and particularly the OH radicals, with fundamental components of bacterial biofilms. © *2014 American Vacuum Society*. [http://dx.doi.org/10.1116/1.4904339]

I. INTRODUCTION

It has become evident that bacterial cells typically live in colonies or a so-called biofilm instead of as free single micro-organisms. A microbial biofilm is an aggregation of microorganisms embedded in a matrix of hydrated extracellular polymeric substances (EPS) and it adheres to both biologic and nonbiologic surfaces.[1] The EPS matrix is mainly composed of polysaccharides, proteins, nucleic acids, and lipids and plays a critical role in the mechanical stability and surface adhesion, as well as in antimicrobial treatments of the biofilm. Studies showed that the formation and integration of biofilms is mainly dominated by polysaccharides present in the EPS matrix. For instance, poly-*N*-acetyl-glucosamine as a polysaccharide in the biofilm of *Staphylococcus epidermidis* plays a critical role in the integrity of the biofilm structure.[1,2]

It is known that the majority of the bacteria found in natural, clinical, and industrial environments are formed as a biofilm on the surface. Clinical studies have revealed the formation and growth of a biofilm in 80% of human microbial infections, such as endocarditis, osteomyelitis, chronic otitis media, foreign-body-associated infections, gastrointestinal ulcers, urinary tract infection, chronic lung infections in cystic biofilms fibrosis patients, caries, and periodontitis.[3] Studies in the field of bacterial treatment show an enhancement in the resistance of bacterial biofilms to antibiotics by a factor of 1000 as compared to antibiotic resistance of single bacteria (planktonic).[4] The main reason of the high resistivity of biofilms to chemical antimicrobial agents, however, has not yet been exactly elucidated, although a number of studies have addressed the considerable effect of the EPS in the impermeability of antimicrobial agents inside the microbial community. For instance, a study on the treatment of biofilms of *Pseudomonas aeruginosa* showed that alginates (as anionic polysaccharides) are capable to bind to positively charged amino glycosides and prevent their penetration into the biofilm.[5] Accordingly, treating the biofilm with conventional methods has become a challenge. Therefore, the development of appropriate alternative techniques for the inactivation of bacterial biofilm is urgently required. In recent years, nonthermal atmospheric pressure plasmas (NTAPP) have shown great potential for the inactivation of bacteria, also in cases where antibiotics are no longer efficient due to natural pathogen and bacterial resistance. Studies on plasma therapy for bacterial treatment have demonstrated the ability of NTAPP to inactivate planktonic bacteria[6–9] and bacterial biofilms,[10–15] as well as to provide an effective method for surface decontamination and sterilization.[16,17]

Additionally, plasmas are of interest for antimicrobial wound treatment, i.e., to disinfect and heal wounds in a contact-free and painless procedure. The antimicrobial properties of NTAPP are mainly attributed to plasma-generated reactive agents, including the neutral particles [e.g., reactive oxygen and nitrogen species (RONS)], charged particles, UV photons, and electromagnetic fields. Especially, the RONS are considered to be able to target cellular components and influence metabolic processes in microorganisms.[18] Plasmas generating these species typically operate at or near room temperature, without being harmful for living tissue. Nevertheless, while NTAPP have proven to eradicate bacterial biofilms, the interaction processes of plasma agents with the biofilm structure are not yet fully understood. Besides experimental studies, atomistic simulations are a useful tool to gain insight into the fundamental aspects of reaction mechanisms of plasma particles with bioorganisms. Comprehensive information about the application of

[a)]Electronic mail: erik.neyts@uantwerpen.be

atomistic simulation methods in plasma medicine context is available in the recent review articles.[19,20]

In this respect, reactive molecular dynamics (MD) simulations were recently applied to investigate the interaction mechanisms of ROS with peptidoglycan (PG) in bacterial cell wall.[21,22] Moreover, the exact penetration mechanisms of ROS (O, OH, HO_2, and H_2O_2) in a liquid layer as the major component of biofilms was examined.[23] Also, reactive MD simulations were used to investigate the interaction of ROS (OH, HO_2, and H_2O_2) with the endotoxic biomolecule lipid A of the gram negative bacterium *Escherichia coli*.[24]

In this study, the reaction mechanisms of hydroxyl (OH) radicals, as one of the most effective ROS in biochemical reactions, with four major groups of organic molecules (alkane, alcohol, carboxylic acid, and amine) surrounded with water was investigated as a model for plasma/biofilm interactions. The simple organic molecules in this investigation are acyclic aliphatic compounds containing ten carbon atoms, viz., decane, decanol, decanoic acid, and decylamine. The importance of studying these molecules is due to the existence of their functional groups in bio-organic molecules, such as lipids, fatty acids, bacterial proteins, and polysaccharides, which are structural components of bacterial biofilms. Furthermore, we also investigate the impact of OH radicals on *N*-acetyl-glucosamine as a saccharide, which has a considerable contribution to the integrity of the *S. epidermidis* biofilm.[2]

II. METHODOLOGY

In our MD simulations, we employed the reactive force field (ReaxFF),[25] using the C/H/O/N glycine/water parameters developed by Rahaman.[26] The parameters for the ReaxFF potential are optimized with respect to quantum mechanical calculations for reaction energies, reaction barriers, and structures. More information on the force field parameters used in this study can be found in references.[26] ReaxFF was developed based on the bond order/bond distance relationship, formally presented by Abell.[27] In this potential, all types of bonding, ranging from covalent to ionic bonding as well as long-range van der Waals forces and Coulomb forces, are taken into account. The molecular charge distribution, based on molecular geometry and connectivity, is calculated using the electronegativity equalization technique.[28,29]

The simulation setup adopted in this work is as follows. An organic molecule is located at the center of the simulation box with dimensions of $25 \times 25 \times 24.38$ Å^3. Periodic boundary conditions are applied in all dimensions. Water molecules were randomly positioned in the empty space surrounding the molecule, until a water density of 1 g cm^{-3} was obtained. Before initiating the OH radical impact, the system is first minimized and then thermalized for 250 ps in the canonical ensemble at room temperature (i.e., 300 K) using the Bussi thermostat.[30] In our simulations, the water-organic molecule system is first equilibrated, and subsequently the OH radical is randomly added to the simulation box. To simulate a dilute solution with an OH mole fraction of 0.002, one OH radical is inserted in the water box containing 500 water molecules and one organic molecule, corresponding to a concentration of about 0.1 M.

III. RESULTS AND DISCUSSION

A. Validation of the force field

We first validated the force field used in our simulations (C/H/O/N glycine/water) by calculating structural, statistical and dynamic properties of pure water including the O-H bond length, the partial charge on the oxygen and hydrogen atoms, the HÔH angle, the water dipole moment, the O-O distance and the radial distribution function. The results show overall a very good agreement with *ab initio* calculations,[31] classical MD simulations,[32] as well as experiments[33–38] (see supplementary material, Fig. 1 and Table I).[39] The validity of the force field to reproduce the hydrocarbon–water complex formation was previously demonstrated for the glycine/system.[26] Furthermore, this force field, in combination with a ReaxFF description for organophosphates, as used by Zhu *et al.*,[40] was successfully applied by Abolfath *et al.*[41] for the simulation water of DNA damage by hydroxyl radicals in solution.[41]

We also examined the applicability of the force field to describe the water–hydroxyl radical system. First, we calculated the diffusion coefficient of OH in a water box from the long-time evolution of the mean squared displacement (MSD), using the Einstein relation:

$$D = \lim_{t\to\infty} \left\langle \frac{|r(t) - r(t_0)|^2}{6(t - t_0)} \right\rangle, \quad (1)$$

where $r(t)$ is the position of the molecule at time t. The MSD was calculated over a 250 ps interval in a 500 ps simulation time. The obtained value for the diffusion coefficient is 0.84 Å^2/ps, which is in good agreement with earlier MD simulations of hydroxyl radicals in water.[42]

Subsequently, in order to further validate the force field for the water-OH radical system, the interaction energy between one OH radical and one water molecule for a certain initial orientation was calculated as[43]

$$E_{WR} = E_{PES} - (E_{H_2O} + E_{OH}), \quad (2)$$

where E_{WR} is the water-radical interaction energy, E_{PES} is the potential energy surface of the water-OH complex, and E_{H_2O} and E_{OH} are the energies of a single isolated water molecule and OH radical, respectively. Following Pabis *et al.*,[43] we calculated the energy profile for a specific configuration, where the water molecule and OH radical lie in the same plane, forming an angle of $\phi = 110°$. The energy profile is plotted in Fig. 1. This figure shows that a minimum energy of -33.21 kJ/mol is found at a distance of $R_{OrOw} = 2.78$ Å. Comparing with the DFT result obtained in Ref. 43 (i.e., predicting a minimum energy of -21.1528 kJ/mol at a distance

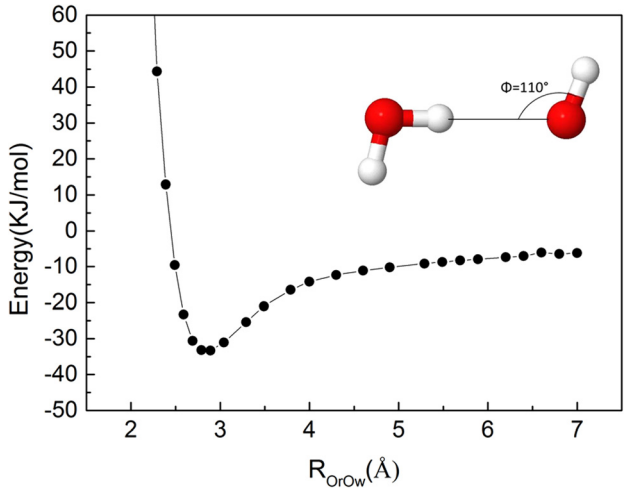

FIG. 1. OH-H_2O interaction energy for the depicted geometry of the complex.

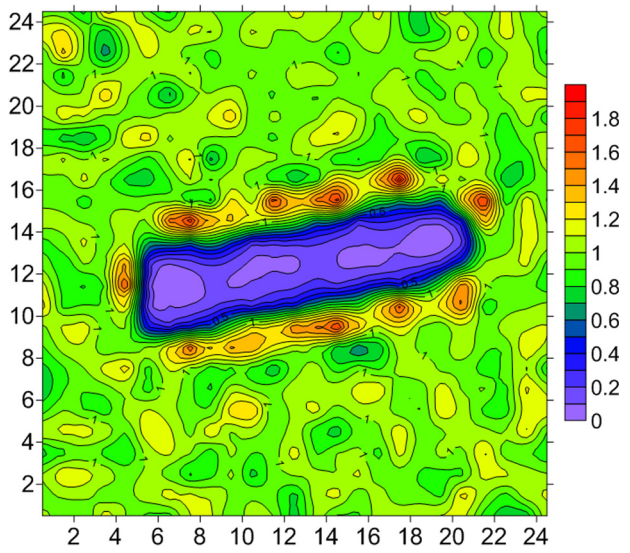

FIG. 2. Contour plot of the water mass density integrated over $z = \{9–14$ Å$\}$, i.e., over the slab in which the organic molecule (decanol) is located.

of 3 Å), it can be concluded that in this case only qualitative agreement is found between ReaxFF and DFT.

Although the main objective of this paper is the investigation of reactions of the OH radical with organic molecules (or biomolecules) in aqueous solution, it is useful to first examine the reaction of OH with the organic molecules to be studied in the gas phase using the above mentioned force field, in order to further validate the force field, by comparison with available experiments from literature. Therefore, we have simulated the reaction of OH radicals with the above mentioned alkane, alcohol, carboxylic acid, and amine in the gas phase.

The observed reaction with these four organic compounds was hydrogen abstraction, leading to the formation of a water molecule and an organic radical, in agreement with experiments.[44] We thus conclude that the force field is suitable for investigating OH/organic molecule chemical reactions.

B. Mass density of water in a box including an organic molecule

In this section, we investigate the mass density of water in the simulation box in the presence of an organic molecule. Here, we consider the alcohol (decanol) as the organic molecule. The molecule was fixed at the center of the simulation box. The mass density of water was calculated by constructing a three dimensional grid with a bin size of 1 Å in the three Cartesian directions and count the number of water molecules in each bin. To enhance the visibility of the effect of the presence of the organic molecule on the local water mass density, the mass density was integrated $z = \{9-14$ Å$\}$, i.e., over the slab in which the molecule is located. The contour plot of the resulting mass density is illustrated in Fig. 2. We have also calculated the mass density as integrated over the entire z-range, as shown in Fig. 2 of the supplementary material. As can be clearly seen, the mass density of water around the organic molecule is slightly increased. We propose the following mechanism. In the bulk of the water (i.e., near the periodic boundaries of the simulation box), the water tends to adopt the normal mass density so as to minimize its free energy. At the interface between the water and the organic molecule, only dipole-induced dipole and London dispersion interactions are present and the water molecules cannot form hydrogen bonds with the alkane chain due to its hydrophobic nature. The organic molecule thus attracts the surrounding water molecules less strongly than the bulk water does. As a result, the water mass density slightly increases in the vicinity of the organic molecule.

C. Trajectory of plasma species in water in the presence of organic molecules

In order to assess the configurational sampling of the water box by a single OH radical in the presence of an organic molecule (again decanol), the trajectories of the OH radical and the organic molecule in the simulation box are calculated and represented as probability profiles. For this purpose, a three dimensional grid with bin size of 1 $Å^3$ is constructed in the simulation box. We recorded the number of times that the OH radical or the functional group of the organic molecule samples any bin, and from these data, the probability is calculated. In Figs. 3(a)–3(d), the profiles for the OH radical are shown, accumulated for total simulation times of 125, 250, 325, and 470 ps, respectively. In these figures, the probability is integrated over every bin in the z-direction and projected onto the $\{xy\}$-plane.

By comparing the probability profiles in Figs. 3(a)–3(d), it can be seen that a more or less complete (albeit not uniform) spatial sampling requires a time scale of about 500 ps. Also, the visiting probability of the hydroxyl group of the organic molecule was determined with the same method as for the OH radical, as shown in Figs. 4(a)–4(d). From this figure, it is concluded that the organic molecule can also travel in

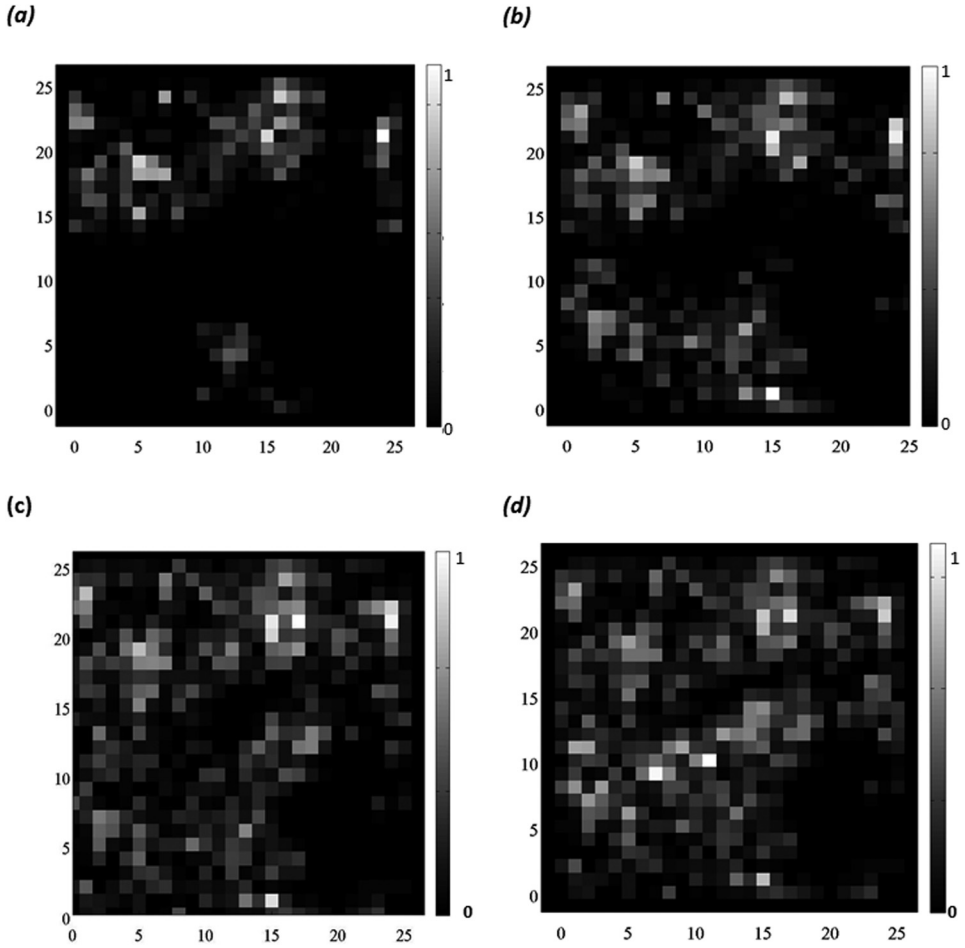

FIG. 3. Trajectories of the OH radical in the simulation box for total simulation times of 125, 250, 325, and 470 ps, shown in (a)–(d), respectively.

the water box, but, in contrast to the OH radical, it is obvious that the organic molecule is transported much more slowly than the OH radical, as it is mainly found in the upper right corner or lower left corner in Fig. 4 (which is reached by the periodicity of the box), but it does not travel within the entire box within this simulation time. The origin for this behavior is twofold. First, the organic molecule is much larger and hence it diffuses more slowly. Second, the OH radical is transported through the water by a fast and continuous chain of chemical H-exchange reactions (see Ref. 23 for more details), instead of pure physical diffusion as is the case for the organic molecule. The high reactivity and fast diffusion of the OH radical has been demonstrated in Ref. 45 as well. In this work it was shown that the OH radicals are very reactive and can reach diffusion lengths of about the diameter of a typical protein.

D. Distance probability of the OH radical in the water/organic molecule box

To gain a better insight into the dynamics of the OH radical in the water box containing the organic molecule, the probability of finding the OH radical at any particular distance from the functional group of the organic molecule is calculated. In Fig. 5(a), the probability of the distance between the OH radical and the (functional group of the) alcohol is plotted. It is clear from this figure that OH can be located at all possible distances from the alcohol. The value of the probability increases with increasing distance up to half the box length, 12.5 Å. This trend is expected due to the cubic box geometry. Indeed, if we consider that the organic molecule is fixed at the center of the box, the probability changes corresponding to the increasing volume of the spherical shells around the center of the box. Therefore, a higher probability is found at a distance equal to half of the box length, where the volume of the spherical shell is largest. Also, it is clear from Fig. 5(a) that the OH radical can be found at a distance below 2 Å from the alcohol, albeit with low probability. It is concluded that in order for a reaction to occur, it is not necessary for the OH radical to remain for a long time close to the organic molecule. Instead, as soon as the radical reaches the vicinity of the reactive part of the organic molecule, the reaction occurs.

The same trend was observed for the density probability between the OH radical and the functional group of the carboxylic acid, the alkane and the amine, as shown in Figs. 5(b)–5(d). However, for the amine and alkane, no reaction occurs, as will be discussed in Sec. III E.

It must be noted that, to obtain statistically valid results for each of the mentioned molecules in the water box, 20

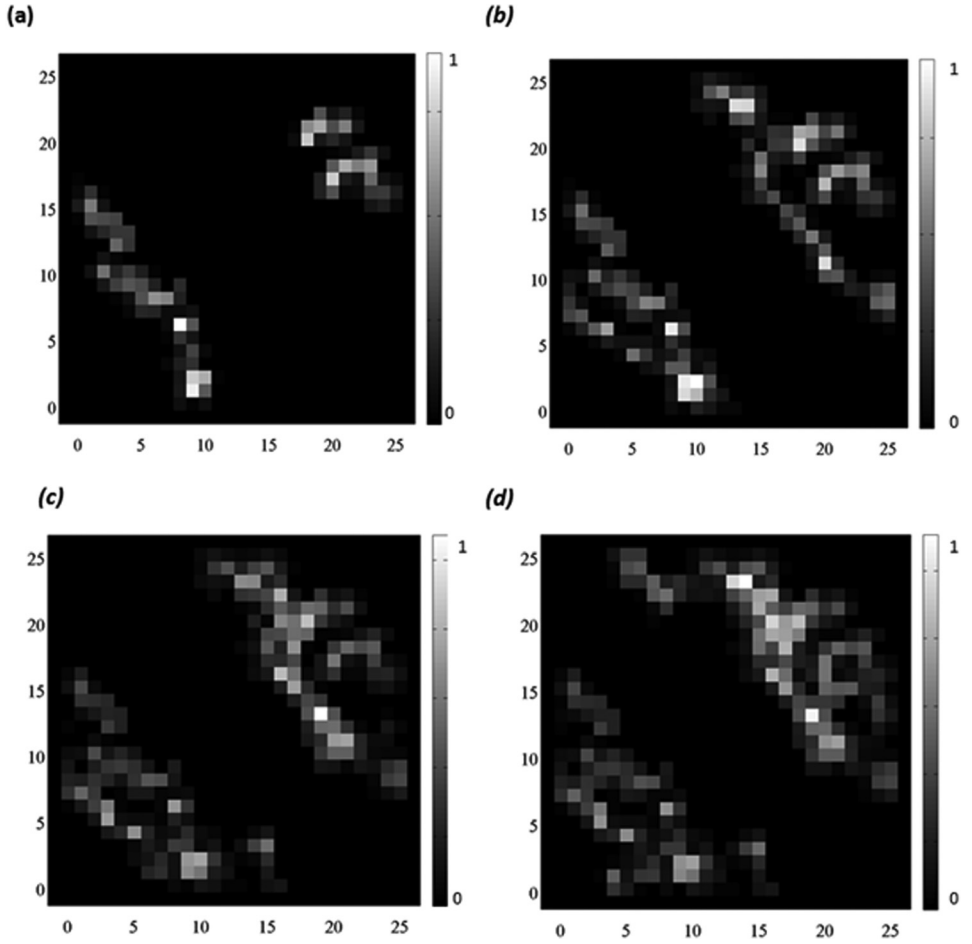

FIG. 4. Trajectories of the hydroxyl group of the organic molecule in the simulation box for total simulation times of 125, 250, 325, and 470 ps, shown in (a)–(d), respectively.

simulations with different initial configurations were carried out. The reaction time of each configuration is different, showing a very large standard deviation, in agreement with the probabilistic nature of the reactions.

E. OH-organic molecule reaction mechanisms in the water box

In this part, the reaction mechanisms of OH radicals with the specific organic compounds (i.e., alkane, alcohol, carboxylic acid, and amine) in the water box are investigated. The reaction mechanism of an OH radical with a dissolved alcohol molecule is presented Figs. 6(a)–6(c). The OH radical is transported randomly through the water box until it reaches the vicinity of the hydroxyl group of the alcohol molecule [Fig. 6(a)]. Then, the OH radical is found to interact immediately with the hydrogen of the alcohol group [Fig. 6(b)]. Finally, the H-atom is abstracted from the alcohol group leaving a H_2O molecule and an R-O radical [Fig. 6(c)].

In the case of reaction of an OH radical with a carboxylic acid molecule in the water box, the same reaction path is observed. As represented in Figs. 7(a)–7(c), the OH radical interacts with the H atom of the carboxyl group and abstracts the hydrogen atom to create a water molecule and the corresponding RCOO radical.

It is known that the reaction of hydroxyl radicals with some organic compounds such as alcohols and carboxylic acids in water is dominated by concurrent addition of the hydroxyl radical to the molecule and hydrogen abstraction from the functional group of the molecule in reference.[46] The reaction mechanism as observed in our MD simulations is indeed consistent with the reaction of OH radicals with a primary acyclic alcohol as observed experimentally.[46]

Finally, it is worth to mention that we performed the same simulation to investigate the impacts of OH radicals in the water box containing an alkane or an amine molecule, but in these cases, no reaction has occurred.

Hence, based on these simulations we can conclude that biomolecules present in the biofilm structure, which contain hydroxyl and/or carboxyl groups such as polysaccharides, lipids, and proteins, can react with OH radicals in plasma-mediated treatment, and the products of these reactions (i.e., the resulting biomolecule radicals) can initiate structural damage in the biofilm. To better understand this interaction process, the impact of OH radicals on a specific polysaccharide (i.e., *N*-acetyl-glucosamine), present in the structure of Staphylococcal biofilm, will be investigated in Sec. III F.

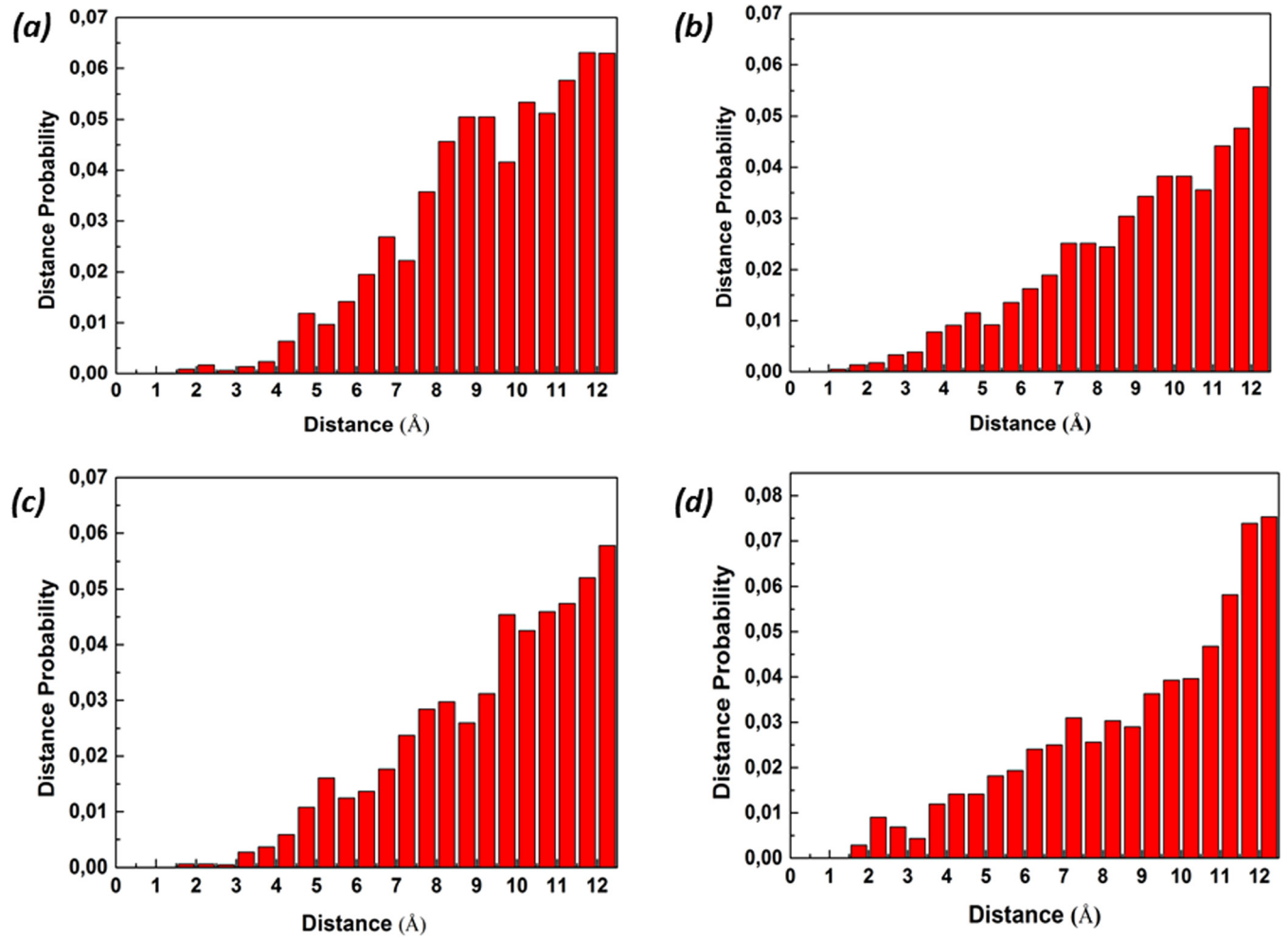

FIG. 5. Probability of distance between the OH radical and the functional group of the alcohol (a), carboxylic acid (b), alkane (c) and amine (d), for total simulation time 470, 455, 500, and 500 ps, respectively.

F. *N*-acetyl-glucosamine

As was explained in the Introduction, polysaccharides are essential components of the biofilm and provide stability of the biofilm structure. They contain several hydroxyl (alcohol, OH) functional groups, which can be attacked by OH radicals due to plasma exposure. To investigate the interaction of OH radicals with a typical polysaccharide, as present in biofilms, we simulated the impact of an OH radical on *N*-acetyl-glucosamine in water, as part of a polysaccharide in the structure of Staphylococcal biofilms.

The important sites of the *N*-acetyl-glucosamine molecule, which can be attacked by the OH radical, are the

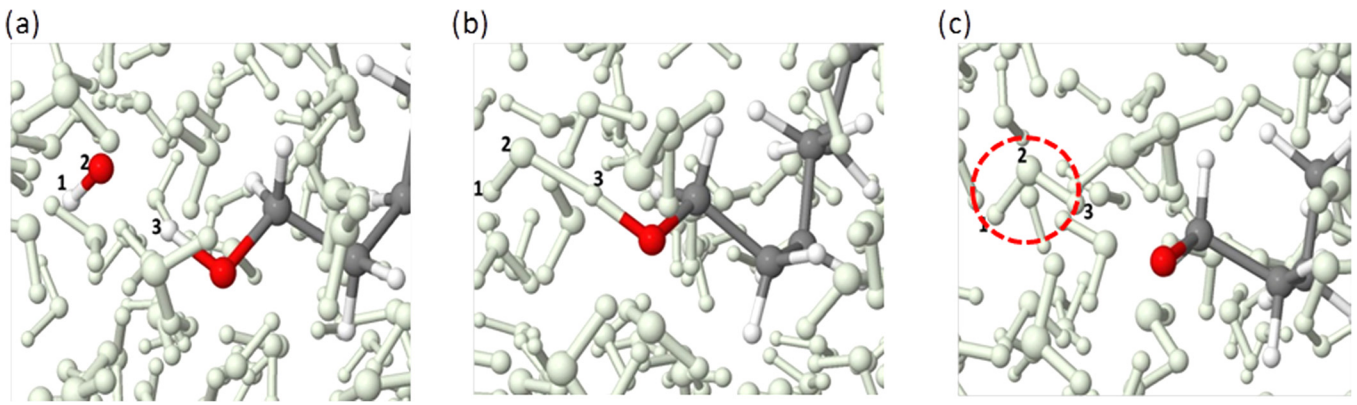

FIG. 6. Snapshots from MD simulations, showing the interaction of an OH radical with decanol in the water box, resulting in the formation of a water molecule and an R-O radical (a)–(c). The newly formed water molecule (i.e., atoms 1, 2, and 3) is shown in the red dashed circle.

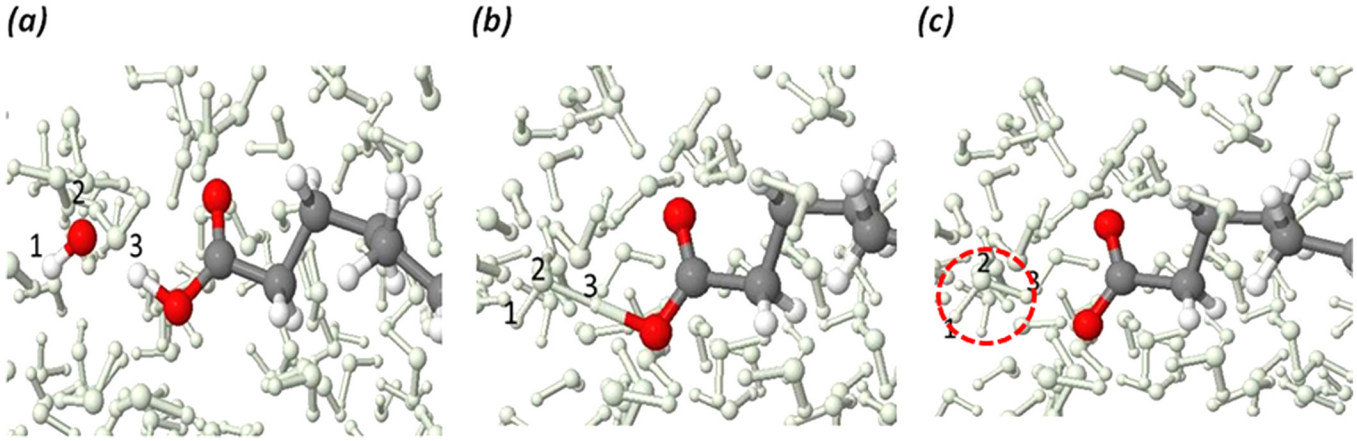

FIG. 7. Snapshots from MD simulations, showing the interaction of an OH radical with decanoic acid in the water box, resulting in the formation of a water molecule and an R-O radical (a)–(c). The newly formed water molecule (i.e., atoms 1, 2, and 3) is shown in the red dashed circle.

hydroxyl groups shown by the dashed circles in Fig. 8(a). Our simulations demonstrate that OH can indeed react with the H atoms from these functional groups.

In this process, hydrogen abstraction from three sites of *N*-acetyl-glucosamine [hydrogen numbers labeled 25, 26, and 27 in Fig. 8(a)] lead to the formation of the same products (i.e., a water molecule and an R-O radical). Also, the bond lengths between the other atoms of *N*-acetyl glucosamine remain unchanged, and the ring remains intact, as shown in Figs. 8(b) and 8(c). In the case, however, that the OH radical abstracts hydrogen number 21, the distance between the O-atom from this hydroxyl group and the attached C-atom [shown in dashed circle line in Figs. 9(a)–9(c)] decreases and leads to the formation of a double C-O bond and subsequently bond cleavage of C-O in the ring [see Fig. 9(c)].

The average bond length of the C = O double bond is found to be 1.18 Å, which is a typical value for a double C = O bond. Hence, we can conclude that the reaction of an OH radical with a polysaccharide (here *N*-acetyl glucosamine) in the biofilm leads to structural damage, depending on the H-atom that is abstracted. In other words, the OH radicals are able to induce instability in the structure of the biofilm by hydrogen abstraction of functional groups (OH) of polysaccharides present in the EPS matrix of the biofilm. For better visualization, the water molecules around the biomolecule were hidden in Figs. 8 and 9. In Figs. 3(a)–3(c) in the supplementary material, the reaction mechanism of an OH radical with *N*-acetyl-glucosamine in water is presented. As shown in Fig. 3(a), the OH radical reaches the vicinity of H21 and abstracts this hydrogen, so as to form a water molecule [dashed circle in Fig. 3(b)]. As explained above, this abstraction leads to ring opening in the *N*-acetyl-glucosamine molecule [see Fig. 3(c)].

IV. CONCLUSIONS

We have investigated the interaction of OH radicals, as key reactive species in chemical and biochemical processes, with typical functional groups of organic molecules (i.e.,

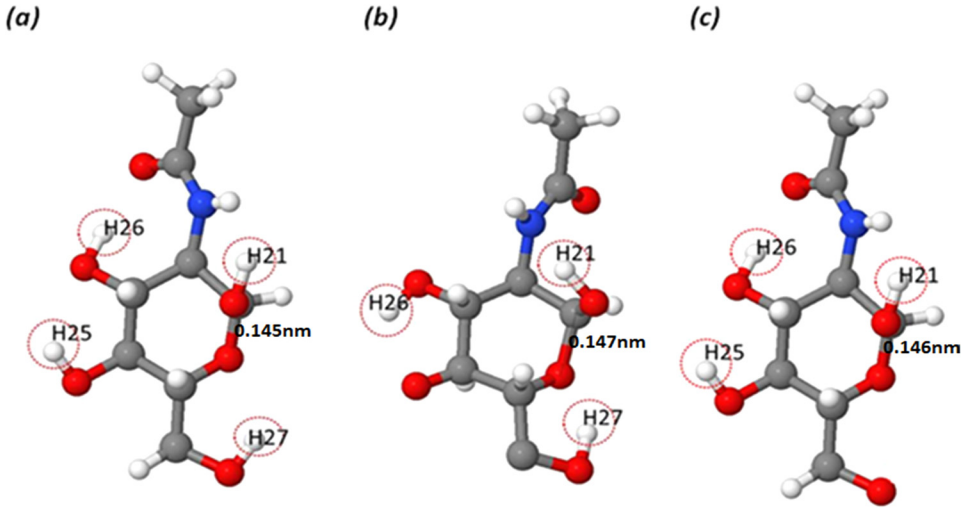

FIG. 8. Snapshots from MD simulations, showing the important sites (hydroxyl groups) of the *N*-acetyl glucosamine molecule, which can be attacked by the OH radical (a). Abstraction of (b) H25 and (c) H27, leaving the ring unchanged.

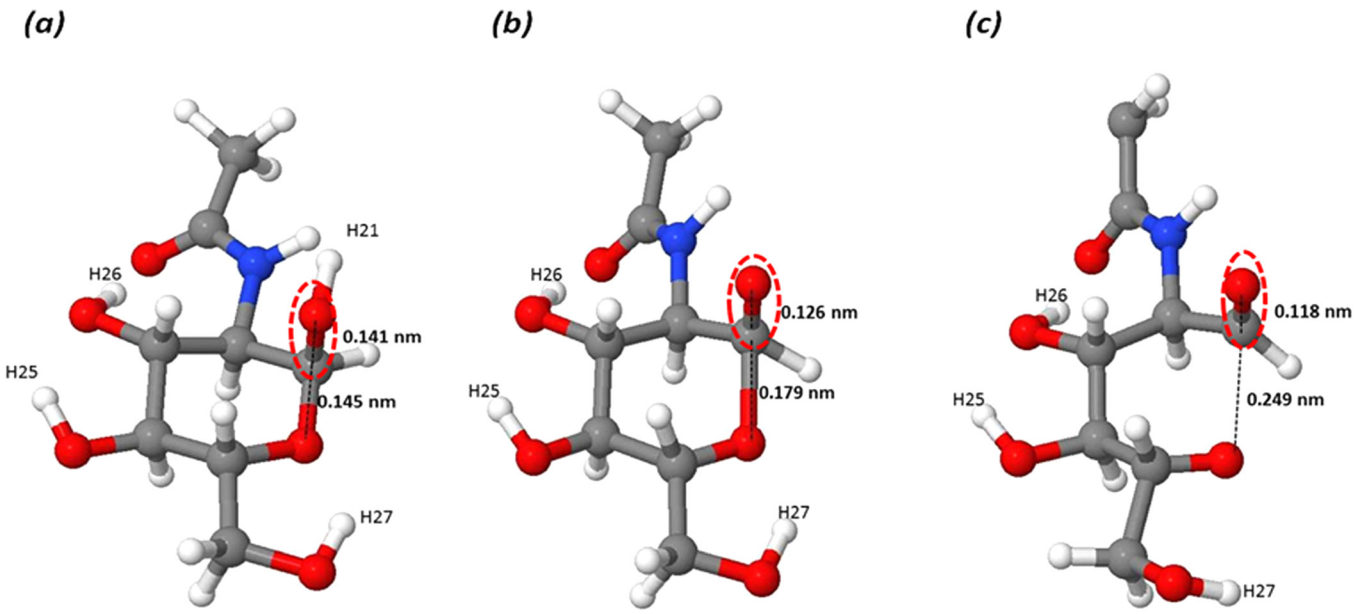

FIG. 9. Snapshots from MD simulations, showing the hydrogen abstraction process (i.e., H21 abstraction) from the *N*-acetyl glucosamine molecule. Following this H-abstraction, the C-O bond length [see red dashed circle in (b)] decreases and leads to the formation of a double C = O bond and subsequently bond cleavage of the C-O bond in the ring (c).

alkane, alcohol, carboxylic acid, and amine), in aqueous solution. We found that OH radicals can only react with the organic molecule after stochastically reaching the vicinity of the functional group. In the case that the organic molecule contains a hydroxyl or carboxyl group, such as in the case of an alcohol and carboxylic acid, the OH radical can interact with the hydrogen of the hydroxyl group and abstract the hydrogen to form a water molecule and an oxyl radical. It is therefore concluded that some organic molecules may act as trapping agents for OH radicals: as soon as they come close to the molecule, they react.

On the other hand, our results show that no reactions occur between OH radicals and saturated alkane and aliphatic amine molecules in water.

Finally, the reaction of OH radicals with *N*-acetyl glucosamine as a saccharide in the biofilm was examined. The simulations show that impact of OH with some specific part of *N*-acetyl-glucosamine leads to bond breaking in the ring and subsequently to structural damage to the polysaccharide in the biofilm.

ACKNOWLEDGMENTS

The authors acknowledge financial support from the Fund for Scientific Research—Flanders (project number G012413N). This work was carried out using the Turing HPC infrastructure at the CalcUA core facility of the Universiteit Antwerpen (UA), a division of the Flemish Supercomputer Center VSC, funded by the Hercules Foundation, the Flemish Government (department EWI) and the UA.

[1]H.-C. Flemming and J. Wingender, Nat. Rev. Microbiol. **8**, 623 (2010).
[2]E. A. Izano, M. A. Amarante, W. B. Kher, and J. B. Kaplan, Appl. Environ. Microbiol. **74**, 470 (2008).
[3]D. Lebeaux, A. Chauhan, O. Rendueles, and C. Beloin, Pathogens **2**, 288 (2013).
[4]J. Costerton, P. S. Stewart, and E. Greenberg, Science **284**, 1318 (1999).
[5]M. C. Walters, F. Roe, A. Bugnicourt, M. J. Franklin, and P. S. Stewart, Antimicrob. Agents Chemother. **47**, 317 (2003).
[6]Y. Ma, G.-J. Zhang, X.-M. Shi, G.-M. Xu, and Y. Yang, IEEE Trans. Plasma Sci. **36**, 1615 (2008).
[7]L. F. Gaunt, C. B. Beggs, and G. E. Georghiou, IEEE Trans. Plasma Sci. **34**, 1257 (2006).
[8]M. Laroussi and F. Leipold, Int. J. Mass Spectrom. **233**, 81 (2004).
[9]E. Kvam, B. Davis, F. Mondello, and A. L. Garner, Antimicrob. Agents Chemother. **56**, 2028 (2012).
[10]N. Abramzon, J. C. Joaquin, J. Bray, and G. Brelles-Marino, IEEE Trans. Plasma Sci. **34**, 1304 (2006).
[11]G. Brelles-Mariño, J. C. Joaquin, J. Bray, and N. Abramzon, *Proceedings of the 2nd International Workshop on Cold Atmospheric Pressure Plasmas* (2005), pp. 69–72.
[12]M. Y. Alkawareek, Q. T. Algwari, S. P. Gorman, W. G. Graham, D. O'Connell, and B. F. Gilmore, FEMS Immunol. Med. Microbiol. **65**, 381 (2012).
[13]M. Y. Alkawareek, Q. T. Algwari, G. Laverty, S. P. Gorman, W. G. Graham, D. O'Connell, and B. F. Gilmore, PloS One **7**, e44289 (2012).
[14]J. C. Joaquin, C. Kwan, N. Abramzon, K. Vandervoort, and G. Brelles-Marino, Microbiology **155**, 724 (2009).
[15]M. H. Lee, B. J. Park, S. C. Jin, D. Kim, I. Han, J. Kim, S. O. Hyun, K.-H. Chung, and J.-C. Park, New J. Phys. **11**, 115022 (2009).
[16]F. Rossi, O. Kylian, H. Rauscher, M. Hasiwa, and D. Gilliland, New J. Phys. **11**, 115017 (2009).
[17]D. Wang, D. Zhao, K. Feng, X. Zhang, D. Liu, and S. Yang, Appl. Phys. Lett. **98**, 161501 (2011).
[18]D. B. Graves, J. Phys. D: Appl. Phys. **45**, 263001 (2012).
[19]E. C. Neyts, M. Yusupov, C. C. Verlackt, and A. Bogaerts, J. Phys. D: Appl. Phys. **47**, 293001 (2014).
[20]A. Bogaerts, M. Yusupov, J. Van der Paal, C. C. Verlackt, and E. C. Neyts, Plasma Processes Polym. **11**, 1156 (2014).
[21]M. Yusupov, E. Neyts, U. Khalilov, R. Snoeckx, A. Van Duin, and A. Bogaerts, New J. Phys. **14**, 093043 (2012).
[22]M. Yusupov, A. Bogaerts, S. Huygh, R. Snoeckx, A. C. van Duin, and E. C. Neyts, J. Phys. Chem. C **117**, 5993 (2013).
[23]M. Yusupov, E. Neyts, P. Simon, G. Berdiyorov, R. Snoeckx, A. van Duin, and A. Bogaerts, J. Phys. D: Appl. Phys. **47**, 025205 (2014).

[24]M. Yusupov, E. C. Neyts, C. C. Verlackt, U. Khalilov, A. C. van Duin, and A. Bogaerts, "Inactivation of the endotoxic biomolecule lipid A by oxygen plasma species: A reactive molecular dynamics study," Plasma Processes Polym. (published online).
[25]A. C. Van Duin, S. Dasgupta, F. Lorant, and W. A. Goddard, J. Phys. Chem. A **105**, 9396 (2001).
[26]O. Rahaman, A. C. van Duin, W. A. Goddard III, and D. J. Doren, J. Phys. Chem. B **115**, 249 (2011).
[27]G. Abell, Phys. Rev. B **31**, 6184 (1985).
[28]W. J. Mortier, S. K. Ghosh, and S. Shankar, J. Am. Chem. Soc. **108**, 4315 (1986).
[29]G. O. Janssens, B. G. Baekelandt, H. Toufar, W. J. Mortier, and R. A. Schoonheydt, J. Phys. Chem. **99**, 3251 (1995).
[30]G. Bussi, D. Donadio, and M. Parrinello, J. Chem. Phys. **126**, 014101 (2007).
[31]M. Sprik, J. Hutter, and M. Parrinello, J. Chem. Phys. **105**, 1142 (1996).
[32]J. C. Fogarty, H. M. Aktulga, A. Y. Grama, A. C. Van Duin, and S. A. Pandit, J. Chem. Phys. **132**, 174704 (2010).
[33]W. Benedict, N. Gailar, and E. K. Plyler, J. Chem. Phys. **24**, 1139 (1956).
[34]S. A. Clough, Y. Beers, G. P. Klein, and L. S. Rothman, J. Chem. Phys. **59**, 2254 (1973).
[35]K. Krynicki, C. D. Green, and D. W. Sawyer, Faraday Discuss. Chem. Soc. **66**, 199 (1978).
[36]Y. Badyal, M.-L. Saboungi, D. Price, S. Shastri, D. Haeffner, and A. Soper, J. Chem. Phys. **112**, 9206 (2000).
[37]R. Bentwood, A. Barnes, and W.-J. Orville-Thomas, J. Mol. Spectrosc. **84**, 391 (1980).
[38]A. Soper, J. Chem. Phys. **101**, 6888 (1994).
[39]See supplementary material at http://dx.doi.org/10.1116/1.4904339 for the calculated radial distribution function for water, the calculated mass density of water in the presence of a biomolecule integrated over the entire z-range, a table comparing water properties as calculated in this work with literature values, and additional MD snapshots showing the interaction between OH and N-acetyl-glucosamine.
[40]R. Zhu, F. Janetzko, Y. Zhang, A. C. van Duin, W. A. Goddard III, and D. R. Salahub, Theor. Chem. Acc. **120**, 479 (2008).
[41]R. M. Abolfath, A. Van Duin, and T. Brabec, J. Phys. Chem. A **115**, 11045 (2011).
[42]M. G. Campo and J. R. Grigera, J. Chem. Phys. **123**, 084507 (2005).
[43]A. Pabis, J. Szala-Bilnik, and D. Swiatla-Wojcik, Phys. Chem. Chem. Phys. **13**, 9458 (2011).
[44]R. Atkinson, J. Phys. Chem. Ref. Data **26**, 215 (1997).
[45]P. Pacher, J. S. Beckman, and L. Liaudet, Physiol. Rev. **87**, 315 (2007).
[46]L. M. Dorfman and G. E. Adams, *Reactivity of the Hydroxyl Radical in Aqueous Solution*, Natl. Stand. Ref. Data Series (Natl. Bur. Stand., U.S., 1973), 46.